Separation and Purification Technology 136 (2014) 27–35

Contents lists available at ScienceDirect

Separation and Purification Technology

journal homepage: www.elsevier.com/locate/seppur

An efficient wet electrostatic precipitator for removing nanoparticles, submicron and micron-sized particles

Tzu-Ming Chen [a,b], Chuen-Jinn Tsai [a,*], Shaw-Yi Yan [b], Shou-Nan Li [b]

[a] Institute of Environmental Engineering, National Chiao Tung University, No. 1001 University Road, Hsinchu 30010, Taiwan
[b] Green Energy and Environment Research Laboratories, Industrial Technology Research Institute, Rm. 109, Bldg. 64, No. 195, Sec. 4, Chung Hsing Rd., Chu Tung, Hsinchu 31040, Taiwan

ARTICLE INFO

Article history:
Received 17 April 2014
Received in revised form 20 August 2014
Accepted 27 August 2014
Available online 6 September 2014

Keywords:
Wet electrostatic precipitator
Deutsch–Anderson equation
Heterogeneous condensation
Particle control

ABSTRACT

An efficient wire-to-plate single-stage wet electrostatic precipitator (WESP) was designed and tested to control nanoparticles, submicron and micron-sized particles emitted from semiconductor manufacturing processes. Tungsten-wires of 0.36 mm in diameter were used as discharge electrodes and a fixed voltage of −15 kV was supplied to generate the electric field and corona ions. Fine water mist at room temperature was used to quench the high temperature exhaust gas to enhance particle condensation growth and improve the collection efficiency of nanoparticles. Experimental results showed that without fine water mist, nanoparticle collection efficiency was 67.9–92.9%, which was greatly enhanced to 99.2–99.7% when the WESP was operated with fine water mist. A predictive method was developed to calculate the particle collection efficiency equation $\eta(\%)$ in the form as $\eta(\%) = [1 - \exp(-\alpha(N_{De})^{\beta} + \gamma)] \times 100\%$, in which α, β and γ are regression coefficients and N_{De} is the Deutsch number. Good agreement was obtained between present predictions and experimental data. For longer term operation, the periodic wall-cleaning water was used to clean discharge electrodes and collection electrodes regularly. In the field tests, the total collection efficiencies ($40 \leqslant d_p \leqslant 8100$ nm) of the WESP were found to maintain greater than 98.7% and 97.3% for continuous operation for 35 and 22 day at fab A and fab B, respectively.

1. Introduction

Silicon-containing chemicals including silane (SiH_4), tetraethyl orthosilicate (TEOS) and dicholorsilane (DCS) etc. are used as chemical precursors for silicon (Si) film in chemical vapor deposition (CVD) processes [1–3]. Residual SiH_4, TEOS and DCS and byproducts such as SiF_4 in the processes are emitted and treated by the local scrubbers of electric thermal or combustion types. Numerous SiO_2 nanoparticles (diameter < 100 nm) and fine particles (diameter < 2.5 μm) are formed in these local scrubbers [4,5]. These sticky and corrosive particles are emitted into the discharge gas of the local scrubbers at a temperature higher than 200 °C but without being properly treated. When emitted to the workplaces and the atmosphere, they may pose adverse effects on human health, ecology and the environment [6–10].

Electrostatic precipitators (ESPs) are used widely in the industry to remove suspended particles from the exhaust gas because of the advantages of low pressure drop and high operating flow rate. They can also be operated at high exhaust temperature while achieving high particle collection efficiency. However in dry ESPs, the accumulation of dust cake on the discharge and collection electrodes results in the decrease in the electrical field strength [11–13], particle re-entrainment caused by rapping [14–16] and back corona [17], which all lead to reduction in particle collection efficiency. In addition, dry ESPs are not suitable to collect particles that are sticky, corrosive, or have high dust cake resistivity. Wet electrostatic precipitators (WESPs) are designed and developed to eliminate the above-mentioned problems by using periodic or continuous scrubbing water to remove deposited particles on the collection electrodes [13,18].

ESPs have a high collection efficiency for fine particles. However, contrary to theory, experimental studies found that collection efficiency decreased with decreasing particle diameter for particle smaller than about 60 nm [19,20]. The low capture efficiency was primarily attributed to partial charging of ultrafine particles [21,22]. Although using the soft X-ray [23] and increasing the applied voltage of the ESPs [20,24] can minimize the partial charging effect and increases the nanoparticle collection efficiency, it may increase power consumption and operation cost.

Nucleated or heterogeneous condensation was applied in condensation particle counters (CPCs) [25] and many air pollution control devices. According to Tsai et al. [26], when the exhaust gas with a temperature higher than 200 °C was quenched with fine

* Corresponding author. Fax: +886 3 5731880.
E-mail address: cjtsai@mail.nctu.edu.tw (C.-J. Tsai).

http://dx.doi.org/10.1016/j.seppur.2014.08.032
1383-5866/

water mist at room temperature in front of the venturi scrubber, the exhaust gas could reach the super-saturation condition. Nanoparticles and submicron particles were grown to micron-sized and the collection efficiency was enhanced. Their results showed that the particle collection efficiency of the venturi scrubber with the water mist system could be enhanced to 40–80% for particles from 50 to 100 nm in diameter and 80–90% for particles larger than 100 nm. Huang et al. [27] added steam before the venturi scrubber and mixed it with waste stream at room temperature. The collection efficiencies of SiO_2 particles from 70 to 500 nm in diameter were enhanced significantly from 50% to 90%. Yang et al. [28] improved a wet flue gas desulfurization (WFGD) system by adding steam into the gas stream at room temperature to remove particles. The collection efficiency of the WFGD system for particles was improved from 25–45% to 45–70% for $CaCO_3$ particles from 70 to 10,000 nm in diameter. The results of these studies indicate that the collection efficiency of submicron particles can be enhanced by nucleated condensation but the enhancement of nanoparticles collection efficiency is not very obvious.

In the literature, there are no studies to enhance the collection efficiency of fine and nano-sized particles by condensational growth in the WESP. In this study, a wire-in-plate WESP employing particle condensational growth method was designed and tested. The fine and nano-sized particle collection efficiency of the WESP was examined with or without fine water mist using laboratory generated particles. For continuous operation, wall-cleaning water was further used to clean collection and discharge electrodes periodically to maintain a high collection efficiency. Long-term field tests of the WESP were further conducted for more than 3 weeks at two semiconductor fabrication plants (or called fabs) where lots of fine and nano-sized SiO_2 particles were emitted.

To facilitate the design of the WESP, a modified equation based on the empirical equations of Lin et al. [21] and Ortiz's et al. [29] was used to predict the particle collection efficiencies which were then validated by present and previous experimental data.

2. Experimental methods

Fig. 1 shows the schematic diagram and dimensions of the present WESP made of stainless steel with a condensation chamber at the inlet. In the condensation chamber, fine water mist (average droplet diameter is 15–20 μm) is generated by atomizer nozzles (Model SU1A, Spraying System Corp., USA) and the mixing ratio is kept at 0.9–0.11 to ensure that nanoparticles and fine particles can grow to 0.8–1.75 μm [26,27].

There are total of four channels in the WESP and four tungsten-wire discharge electrodes of 0.36 mm in diameter in each channel. The channel width is 0.048 m. The surface area of each collection electrode is 0.034 m^2. To generate the electric field and corona ions, −15 kV was supplied on the discharge electrodes by using a high voltage power supply (Model PT-10, Taiwan-ep Corp., Taiwan). The distances of discharge wire to the collection electrode and the wire to wire are 24 and 56 mm, respectively. In order to clean collection and discharge electrodes, two spray nozzles (Model Flat Jet K, Spraying System Corp., USA) were installed at the top of each collection electrode to spray clean water on the wall and wires at a wide-angle of 115–120°. For water saving, the cleaning duration was 10 s for every 10 min at the water flow rate of 0.6 L/min for each collection electrode. During cleaning, high voltage power was disconnected to avoid short circuiting.

Fig. 2 shows the experimental setup for the tests in the laboratory and at field. An electrical low pressure impactor (ELPI, Dekati Ltd., Finland), which combines the well-known impactor technology with particle charging and electrical detection and enables real-time particles size distribution measurements (size range of

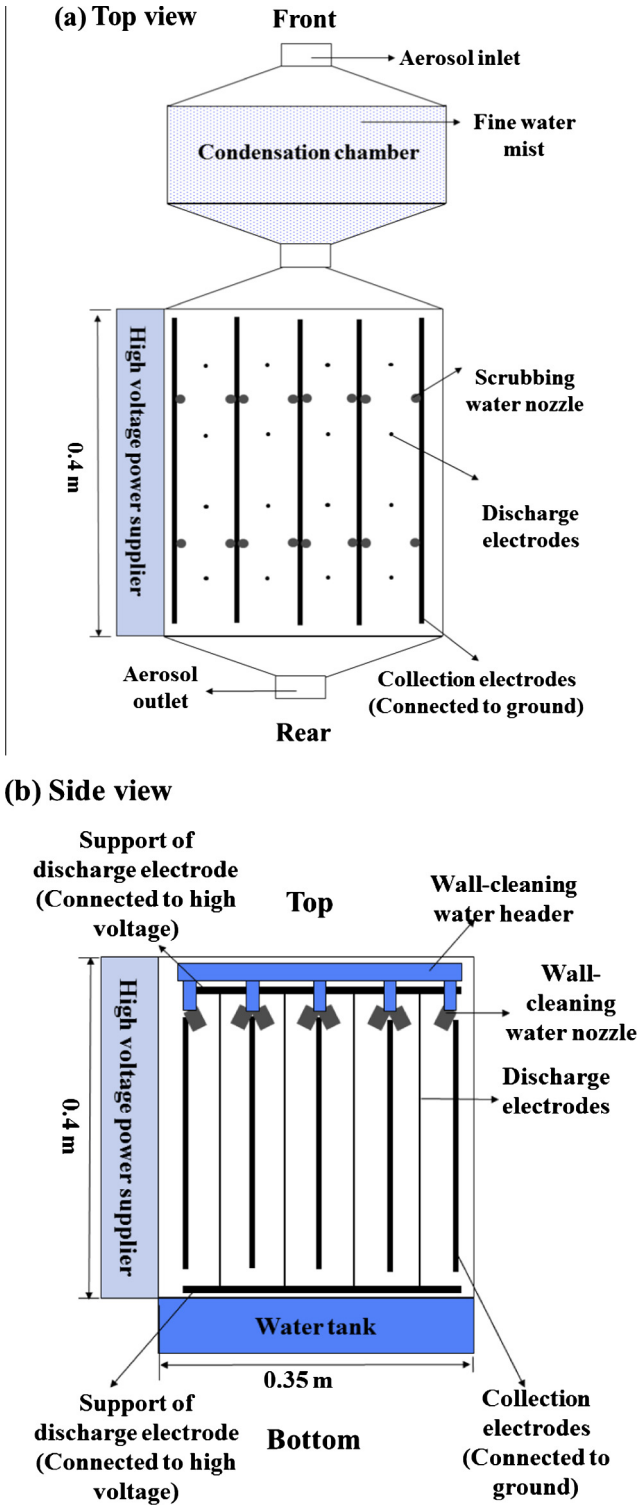

Fig. 1. Schematic diagram of the present WESP. (a) Top view and (b) side view.

30–10,000 nm), was employed to measure the size distributions at the WESP inlet and outlet. The particle collection efficiency (η_{dp}) is calculated by the following equation:

$$\eta_{dp}(\%) = \frac{C_{in}(d_p) - C_{out}(d_p)}{C_{in}(d_p)} \times 100\% \quad (1)$$

where $C_{in}(d_p)$ is the inlet particle concentration and $C_{out}(d_p)$ is the outlet particle concentration for particles with the diameter d_p.

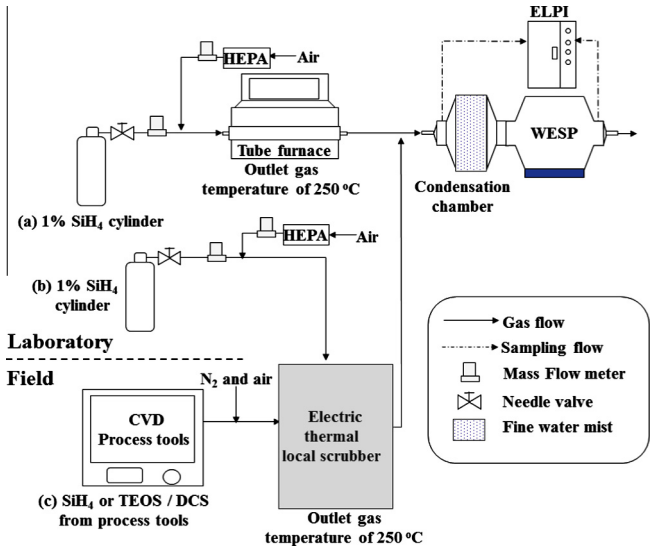

Fig. 2. Schematic diagram of the experimental setup. (a and b) Laboratory tests, (c) field tests.

At first, laboratory tests for particle collection efficiency were conducted when the present WESP was initially clean and with or without fine water mist for particle condensational growth (in part (a) of Fig. 2). 1% SiH_4 from a cylinder was oxidized by the tube furnace to generate polydisperse SiO_2 particles for the tests. Mass flow meters were used to control the carrier air and SiH_4 gas flow rates. The gas temperature at the inlet of the WESP was measured to be 250 ± 20 °C, which is close to the exhaust gas temperature of an electric thermal local scrubber commonly used in fabs. The air velocities of 0.062, 0.093 and 0.124 m/s corresponding to the residence time of 3.95, 2.63 and 1.79 s were used for the tests.

Prior to long-term field tests, the particle collection efficiency of the present WESP was tested continuously for 1 week (operating for 6 h each day), using aerosols generated from an electric thermal local scrubber (Model SGA-310, IPI, Taiwan) in the laboratory as shown in part (b) of Fig. 2. 1% SiH_4 from a cylinder was oxidized by the local scrubber to generate polydisperse SiO_2 particles. Long-term operation of the WESP was then continued for 22 and 35 days at fabs A and B, respectively, in the Hsinchu Science Park, Taiwan (part (c) of Fig. 2). Chemicals discharged from upstream process tools including SiH_4 in fab A, and tetraethyl orthosilicate (TEOS) and Dicholorsilane in fab B, were treated by local scrubbers (fab A: Model SGA-310, IPI, Taiwan; fab B: Model Thermal Wet, CDO, USA) and SiO_2 particles were generated. The ELPI was also used to determine the particle collection efficiency at the 7th day and the end of the continuous operation (or 22nd and 35th day) at fab A and B, respectively. Since the field studies were mainly aimed at long-term tests, measurements at the first day were not conducted as requested by fab engineers.

3. Theoretical model

The ideal theoretical equation to predict the particle collection efficiency for the ESP is the Deutsch–Anderson [30] as shown below:

$$\eta(\%) = [1 - \exp(-(N_{De})] \times 100\% \quad (2)$$

where N_{De} is the Deutsch number, which is defined as:

$$N_{De} = \frac{w \cdot A}{Q} \quad (3)$$

where A is the surface area of the collection electrode (m^2), Q is the air flow rate (m^3/s), and w is the particle migration velocity (m/s).

Ortiz et al. [29] developed a simple fitted model which considered several dimensionless parameters, including turbulence and electro-hydrodynamics factors, and a modified N_{De}':

$$\eta(\%) = [1 - 1.042 \times \exp(-(N'_{De})^{0.612}] \times 100\% \quad (4)$$

$$\text{where } N'_{De} = \frac{w}{v} \times \frac{x}{D}; \quad 0 \leqslant x \leqslant L \quad (5)$$

where x is the coordinate in the direction of the air stream, D is the distance of wire to plate (m), v is gas velocity (m/s), L is the collection electrode length (m).

However the best fit to the experimental data [29] by Eq. (4) only applied to particles with the diameter larger than 10 μm. For smaller particles, Lin et al. [21] developed a semi-empirical equation for predicting the collection efficiency as:

$$\eta(\%) = [1 - \exp(-a(N_{De})^b + c(N_{De})] \times 100\% \quad (6)$$

where a, b and c are regression coefficients. Good agreement was obtained at the applied voltage of 35 kV and the gas velocity of 1.41 m/s with the deviation 0.7–5.9% for particles from 0.1 to 10 μm in diameter when $0.15 \leqslant N_{De} \leqslant 2.20$ [21]. As will be shown in the later sections, this equation is not applicable when the gas velocity is lower than 1 m/s and N_{De} exceeds 2.20. In this study, the following modified equation was found to fit present and previous experiment data well:

$$\eta(\%) = [1 - \exp(-\alpha(N_{De})^\beta + \gamma)] \times 100\% \quad (7)$$

where α, β and γ are regression coefficients, which are 1.89, 0.50 and −0.01 respectively. N_{De} is defined in Eq. (3) in which the particle migration velocity w is given by:

$$w = \frac{n_p(t) E_{ave} C(d_p)}{3\pi\mu d_p} \quad (8)$$

In the above equation, E_{ave} is the average electric field strength, $C(d_p)$ is the slip correction factor of particles with d_p (m), μ is the dynamic air viscosity (kg/s m) and $n_p(t)$ is the total number of elemental units of particle charges as a function of time, which can be calculated as [31]:

$$n_p(t) = n_{diff}(t) \times \exp[a_1 \times n_{diff}(t)^{a_2} + a_3 n_{diff}(t) + a_4] + n_{field}(t) \quad (9)$$

where

$$n_{diff}(t) = \frac{d_p kT}{2K_E e^2} \ln\left(1 + \frac{\pi K_E d_p \bar{c}_i e^2 N_i t}{2kT}\right) \quad (10)$$

$$n_{field}(t) = \left(\frac{3\varepsilon}{\varepsilon + 2}\right)\left(\frac{E_{ave} d_p^2}{2K_E e}\right)\left(\frac{\pi K_E e Z_i N_i t}{1 + \pi K_E e Z_i N_i t}\right) \quad (11)$$

where n_{diff} and n_{field} are particle charges acquired due to diffusion and field charging mechanisms, respectively.

In above equations, a_1 is 1.91588, a_2 is −0.1425, a_3 is 1.296×10^{-5}, and a_4 is −1.2671, k is the Boltzmann constant (1.38×10^{-23} J/K), $K_E = 9.0 \times 10^9$ (N m/C^2), e is the elementary charge (C), $\bar{c}_i$ is the mean thermal speed of ion (m/s), Z_i is ion mobility (m^2/V s), ε is the relative permittivity of particle, t is the residence time of particles in ESPs (s). The average ion concentration (N_i, #/m^3) is calculated as:

$$N_i = \frac{J_p}{Z_i E_{ave} e} \quad (12)$$

where J_p is the average current density at the plate (A/m^2), which is defined as:

$$J_p = \frac{I}{4S_x l} \tag{13}$$

where I is total ion current (A) per discharge wire, S_x is the distance of discharge wire to wire (m), l is the wire length (m). The average electric field strength E_{ave} and total ion current I in the present model are calculated by the procedure described in Lin et al. [21].

4. Results and discussion

4.1. Particle collection efficiency of the present WESP

Fig. 3 shows the collection efficiency of the present WESP as a function of particle diameter ($30 \leqslant d_p \leqslant 10{,}000$ nm) when the gas velocity is 0.062 m/s and total particle concentration is 5.0–6.0 $\times 10^6$ #/cm^3 with and without fine water mist. Each condition was tested for 12–15 times. The standard deviation of the data for the condition "without fine water mist" and "with fine water mist" is 1–3.4% and 1–2.0%, respectively. As shown in the figure, the average particle collection efficiency for particles smaller than 100 nm (nanoparticles) is 67.9–92.9% and that for particles larger than 0.1 μm is greater than 99% for the WESP without fine water mist. With water mist, the collection efficiency is significantly improved to 99.2–99.7% for nanoparticles.

In this study, the exhaust gas temperature was measured to be 230–250 °C and fine water mist at room temperature quenched the exhaust gas to 50–60 °C to reach the super-saturation condition so that nanoparticles grew to larger sizes to enhance the collection efficiency. According to Tsai et al. [26], when the mixing ratio was 0.9, nanoparticle could grow to 800–1700 nm depending on particle concentration. From the experimental data, it can be concluded that heterogeneous nucleation and condensational particle growth by fine water mist in the current WESP is effective for nanoparticle removal.

With fine water mist, the experimental average collection efficiencies for particles in the range of $30 \leqslant d_p \leqslant 10{,}000$ nm are greater than 99% at 0.062 m/s, 98.5–99.6% at 0.093 m/s and 95.6–96.9% at 0.124 m/s when the average total particle concentration ranges from 5.0 to 6.0 $\times 10^6$ #/cm^3 as shown in Fig. 4(a)–(c). The standard deviation shown in Fig. 4(a)–(c) is 0.5–1.8%, 0.9–1.6%, and 0.7–2.6%, respectively. It is seen that the collection efficiency drops with increasing gas velocity, or decreasing particle residence time in the present WESP. U-shaped collection efficiency curves are also observed with the minimum collection efficiency corresponding to the particle diameter between 210 and 330 nm, which is similar to that in Lin et al. [13] and Saiyasitpanich et al. [32].

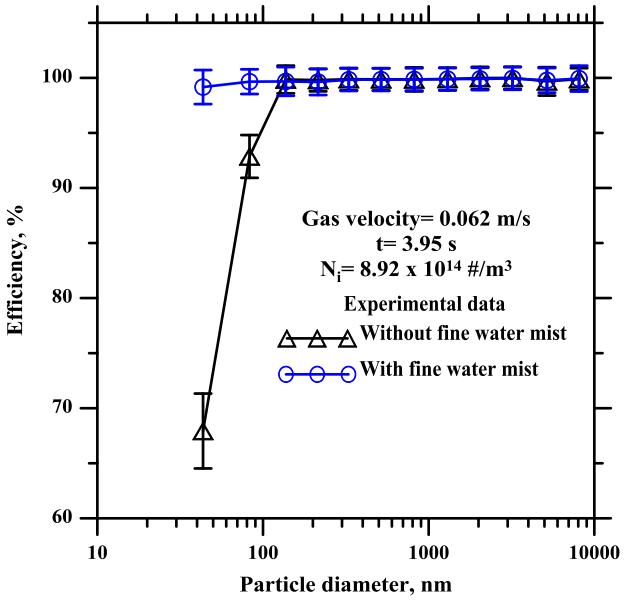

Fig. 3. Collection efficiency of the present WESP with and without fine water mist. The gas velocity is fixed at 0.062 m/s and the applied voltage is −15 kV.

According to particle charging theory, field charging is the main mechanism for particles larger than 1.0 μm in diameter while diffusion charging is the principal mechanism for particles less than about 300 nm [33]. Particle charges acquired due to field charging is particle surface area dependent. Therefore, the increase in the particle charge is proportional to the particle diameter. In diffusion charging dominated regime, the particle charge decreases with decreasing particle size while the mechanical mobility increases rapidly with decreasing particle size. Therefore, there is minimum collection efficiency for ESPs in the particle size range of 100–1000 nm.

4.2. Comparison of experimental particle collection efficiencies with present model results

Fig. 4 also shows the theoretical predictions by the present model, or Eq. (7). The regression coefficients are obtained from experimental data at the gas velocity of 0.124 m/s and the fixed applied voltage of −15 kV when the negative ion mobility is set to be 1.57 $\times 10^{-4}$ m^2/V s [20], which are 1.89 for α, 0.50 for β, and −0.01 for γ, respectively. Particle collection efficiencies were calculated at other operation conditions and compared with the present and previous experimental data [11,17,20,34]. As shown in Fig. 4, for N_{De} in the range from 2.46 to 31.8 (corresponding to particles of $30 \leqslant d_p \leqslant 10{,}000$ nm), the comparison of particle collection efficiencies between present model predictions and present experimental data shows good agreement with a deviation of 0.2–1.1%, 0.3–1.8% and 0.04–2.2% at the gas velocity of 0.062, 0.093 and 0.124 m/s, respectively.

The comparison of predicted particle collection efficiencies by the present model and the model of Lin et al. [21] (Eq. (6)) with previous experimental data in the literature [11,17,20,34] is shown in Fig. 5. In Fig. 5(a) the experimental data of Huang and Chen [11,20] are for particles ranging from 34 to 1000 nm at the fixed gas velocity of 0.18 m/s and the applied voltages of −26.4 kV and −34.5 kV. The predicted values of the present model agree reasonably with experimental data with a deviation of 0.02–4.7% at −26.4 kV and 0.9–5.3% at −34.5 kV. In comparison, the deviation of particle collection efficiencies calculated by Eq. (6) from the experimental data at −26.4 kV and −34.5 kV is much larger, which is 8.5–13.3% and 7.4–10.4%, respectively. If the equation of Ortiz et al. [29] (Eq. (4)) is used, an even larger deviation occurs, which is 23.3–42.0% and 28.5–34.2% at −26.4 kV and −34.5 kV (data are not shown).

Fig. 5(b) shows the ESP efficiency data of Riehle and Löffler [34] at the gas velocity of 0.5 m/s, the applied voltage of −25 kV, and the particle diameter of $300 \leqslant d_p \leqslant 7800$ nm. The prediction of present model is seen consistent with the experimental data with a deviation of 0.3–3.2%. The deviation of the particle collection efficiencies calculated by Eq. (6) from the experimental data is again larger, which is 1.4–11.3%. If Eq. (4) is used, even a larger deviation occurs (data not shown).

Fig. 5(c) shows the comparison of predicted particle collection efficiencies with the experimental data of Chang and Bai [17] at the gas velocity of 0.199 m/s and the applied voltages of −27 kV. The test particle diameter range is $21 \leqslant d_p \leqslant 5550$ nm. The predictions again agree well with the experimental data with a deviation of 0.2–5.8%. The deviation of particle collection efficiencies calculated by Eq. (6) from the experimental data is larger, which

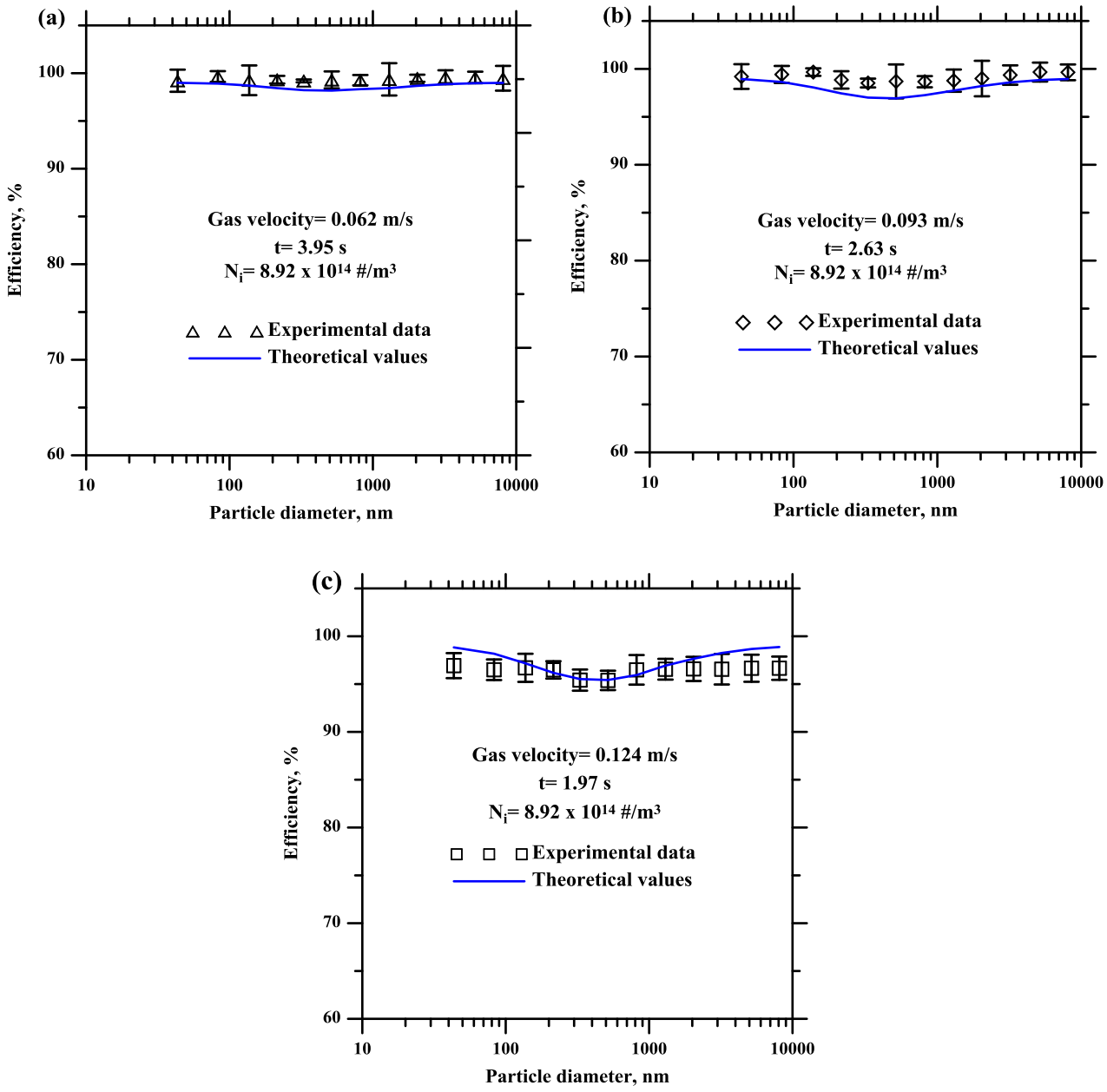

Fig. 4. Comparison of particle collection efficiency of the WESP with fine water mist between the experimental data and the present predictions at the gas velocity of 0.062–0.124 m/s and applied voltage of −15 kV.

is 5.0–13.4%. If the equation of Eq. (4) is used, again a larger deviation occurs (data are not shown).

The comparison of predicted particle collection efficiencies of the present model with present and previous experimental data shows good agreement with a maximum deviation less than 6%. It suggests that present model is appropriate for predicting particle collection efficiency when the gas velocity in the WESP is lower than 0.5 m/s, the particles size range is $30 \leqslant d_p \leqslant 10{,}000$ nm, and N_{De} ranges from 0.72 to 31.81.

4.3. Effect of wall-cleaning water on the collection efficiency of the WESP with fine water mist

To show the effect of particle loading and wall-cleaning water on the collection efficiency of the WESP, SiO_2 particles were generated in the laboratory with the average particle concentration of 7.0×10^6 #/cm^3 and the size range of 40–8100 nm to test the present WESP without wall-cleaning water first at a gas velocity of 0.124 m/s and an applied voltage of −15 kV for 20 min. The average collection efficiencies for particle 40–8100 nm are 93.4–99.9% in average with the standard deviation of 0.8–4.0%, 85.0–99.0% with the standard deviation of 0.7–3.0%, 15.7–39.0% with the standard deviation of 2.0–5.2% and 5.0–21.0% with the standard deviation of 5.0–11.5% at the initial condition, and continuous operation time of 10, 15 and 20 min, respectively, as shown in Fig. 6. The collection efficiency decreased only slightly from 93.4–99.9% to 85.0–99.0% after continuous operation for 10 min. However, after 15 and 20 min, the collection efficiencies decreased substantially to 15.7–39.0% and 5.0–21.0%. A significant amount of SiO_2 particles accumulated on the collection electrodes and discharge wires were observed, which led to the decrease in the collection efficiency due to the decrease in the electric field. In

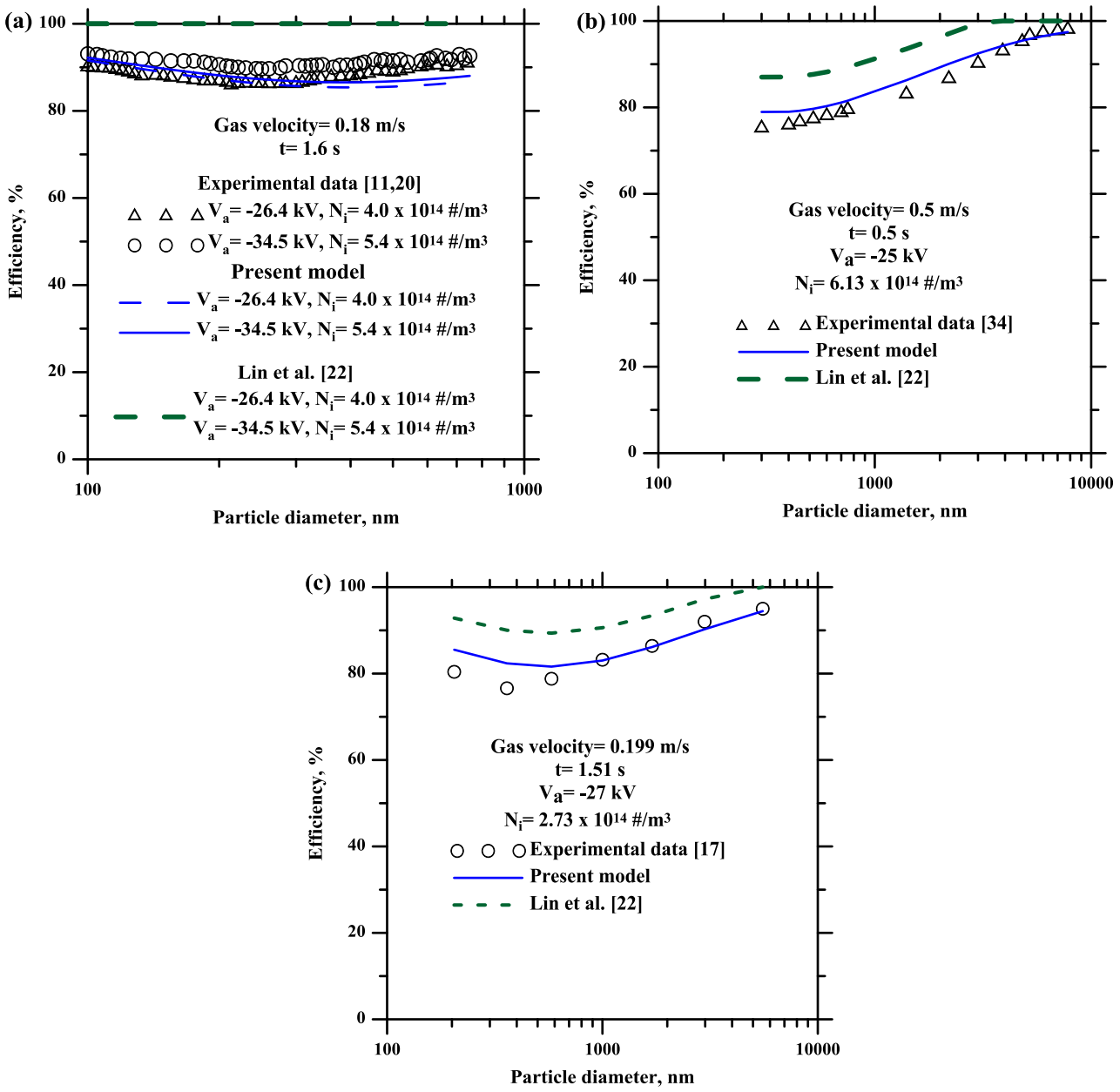

Fig. 5. Comparison of predicted particle collection efficiencies with the experimental data of (a) Huang and Chen [11,20], (b) Riehle and Löffler [34], and (c) Chang and Bai [17].

addition, if the dust cake is too thick, particles could also be re-entrained into the gas stream because of the reduction of the electrostatic force between the SiO_2 dust layer and the collection plate. These re-entrained particles are too small to settle by gravity and might not be captured by dry ESP [35].

With the application of wall-cleaning water to maintain the collection electrodes and wires clean, the collection efficiency of the WESP was measured to be 95.8–98.8% in average with the standard deviation of 0.1–1.5%, 95.0–97.4% with the standard deviation of 0.4–2.1% and 93.1–96.9% with the standard deviation of 0.5–2.7% at the initial condition, and after continuous operation for 1 and 6 h, respectively, as shown in Fig. 7. That is, the collection efficiency does not change very much from the initial condition after long-term operation for up to 6 h. The periodic wall-cleaning water of 0.6 L/min per collection surface area (0.0343 m^2) was found to be able to keep both collection and discharge electrodes clean. Therefore, this laboratory loading test shows that a high collection efficiency of the present WESP can be maintained with the aid of periodic wall-cleaning water spray.

4.4. Long-term field test results

Long-term field tests were conducted at fab A and fab B. At fab A, the WESP was tested at the gas velocity of 0.10–0.11 m/s and the WESP with fine water mist and wall-cleaning water was applied periodically (10 s for every 10 min) at the water flow rate of 0.6 L/min per collection surface area from April 20 to May 25 in 2011 and the particle collection efficiencies were measured at the 7th and 35th day (note: these test dates were requested by the fab engineers) when the total inlet particle concentrations were measured to be 1.2×10^7 #/cm^3 and 1.5×10^7 #/cm^3, respectively. Fig. 8(a) shows the particle number concentration versus particle diameter in the field tests at fab A. As shown in Fig. 8(b), the collection efficiency decreases slightly to 98.1–99.0% after

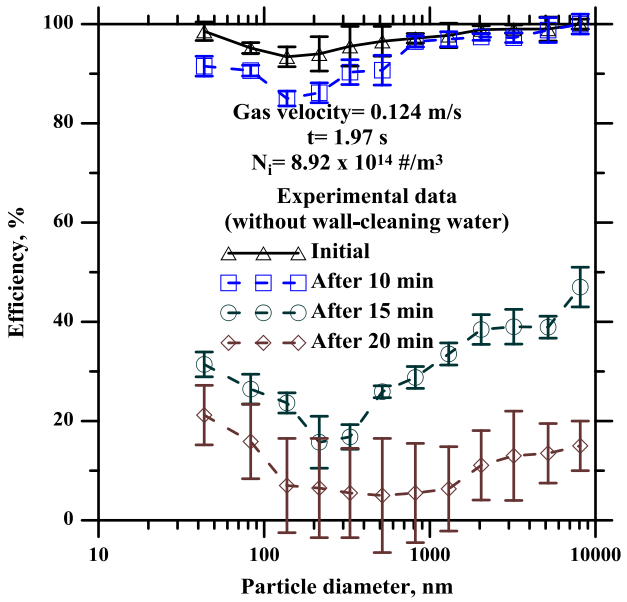

Fig. 6. Collection efficiency of the WESP without wall-cleaning water versus operation time. The applied voltage and gas velocity are −15 kV and 0.124 m/s, respectively.

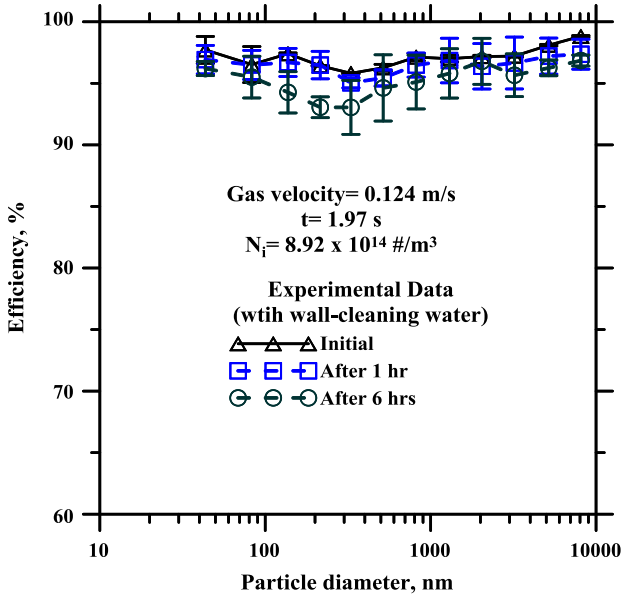

Fig. 7. Collection efficiency of the WESP with wall-cleaning water versus operation time. The applied voltage and gas velocity are −15 kV and 0.124 m/s, respectively.

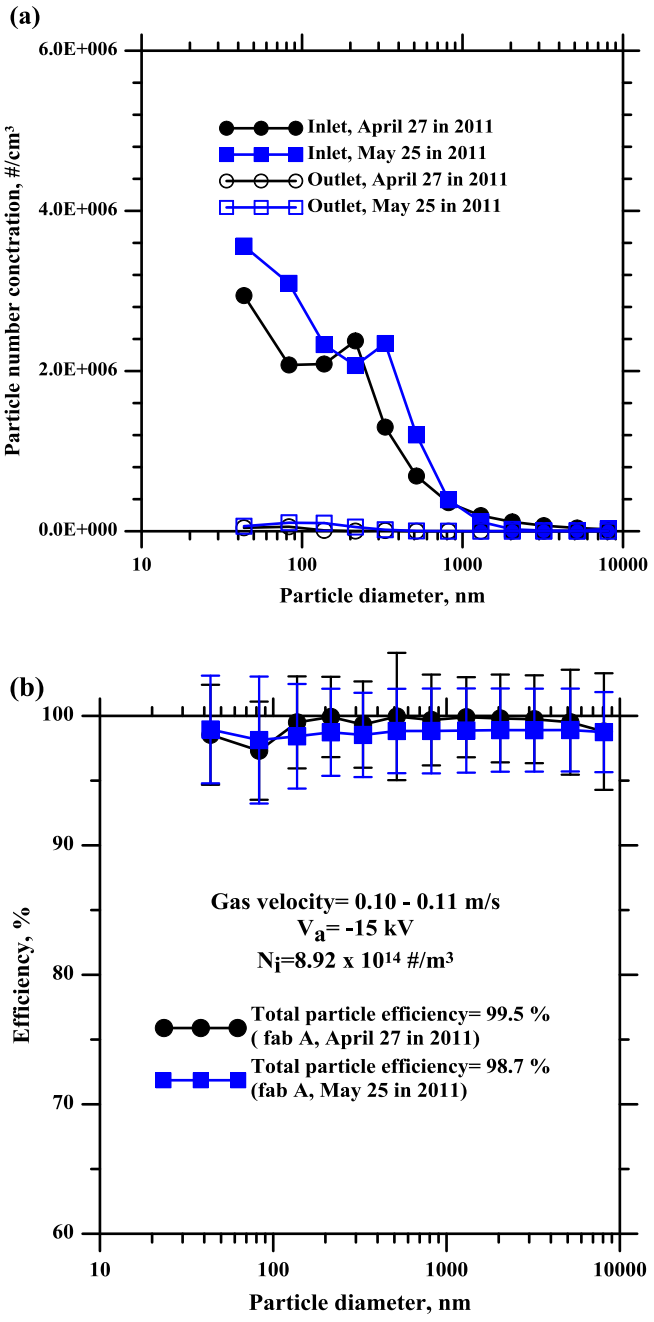

Fig. 8. (a) The particle number concentration versus particle diameter in the field tests at fab A. (b) Total particle collection efficiency of the WESP with fine water mist and wall-cleaning water. WESP 1: gas velocity = 0.10–0.11 m/s, t = 2.4–2.2 s, from April 20 to May 25 of 2011 at fab A.

35-day continuous operation, which is similar to the collection efficiency of 98.5–99.7% at the 7th day. In Fig. 8(b), the standard deviation of the data in "April 27 in 2011" and "May 25 in 2011" is 3.1–5.0%, and 3.1–4.9%, respectively.

The field test at fab B was conducted at the gas velocity of 0.12–0.14 m/s, the applied voltage of −15 kV and the periodic wall-cleaning water of 0.6 L/min per collection surface area (10 s for every 10 min). The total inlet particle concentration was 1.7–1.8 × 10^7 #/cm^3 and the test period was from December 28 of 2012 to January 18 of 2013. The particle collection efficiencies were evaluated at the 7th and 22nd day (note: these test dates were also requested by the fab engineers). Fig. 9(a) shows the particle number concentration versus particle diameter in the field tests at fab B. As shown in Fig. 9(b), the collection efficiency decreases slightly to 97.5–98.4% after continuous operation for 22 days, which is comparable to the collection efficiency of 96.5–99.3% at the 7th day. The standard deviation of the data in "January 2 in 2013" and "January 18 in 2013" is 3.1–4.7%, and 3.2–4.6%, respectively.

These field test results conclude that wall-cleaning water is able to maintain both discharge and collection electrodes clean and ensure that the present WESP with fine water mist can operate at a high particle removal efficiency for long-term.

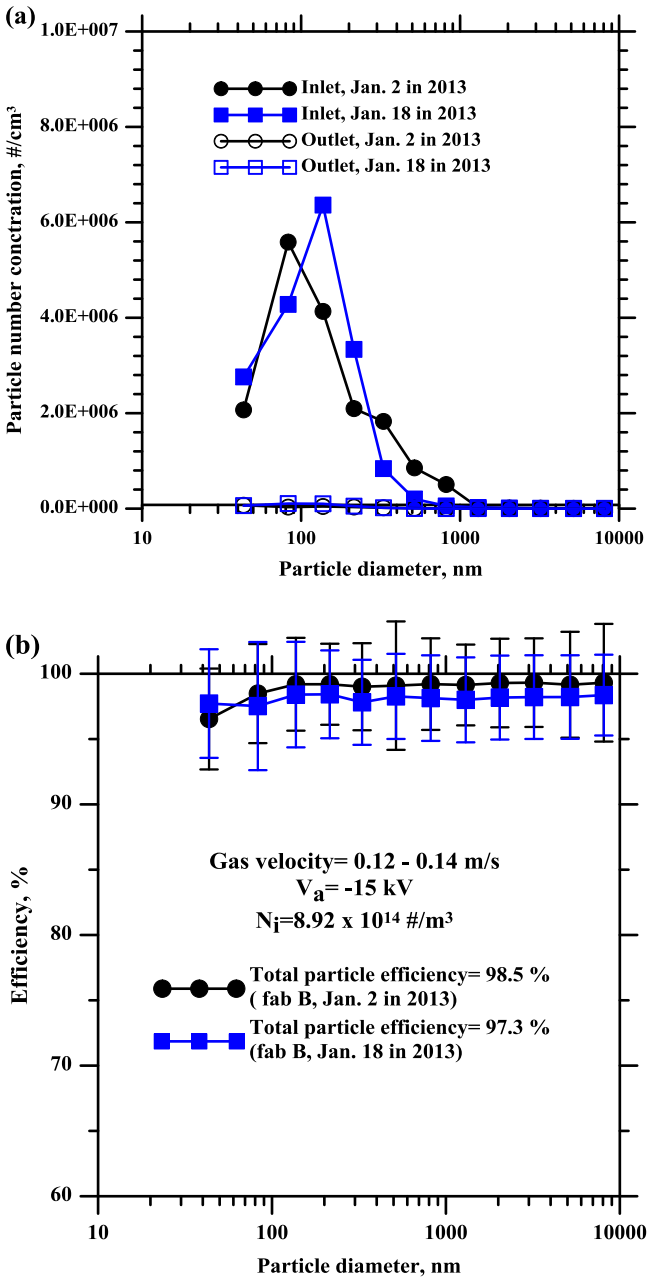

Fig. 9. (a) The particle number concentration versus particle diameter in the field tests at fab B. (b) Total particle collection efficiency of the WESP with fine water mist and wall-cleaning water. WESP 2: gas velocity = 0.12–0.14 m/s, t = 1.97–1.8 s, from December 28 of 2012 to January 18 of 2013 at fab B.

5. Conclusion

This study designed and developed a WESP to control micron, submicron and nano-sized particles. Fine water mist was used to quench high temperature exhaust gas to reach the super-saturation condition to promote condensational growth of nano-particles and enhance their collection efficiency. The experimental results showed that the present WESP can collect particles ($40 \leqslant d_p \leqslant 8100$ nm) efficiently at the applied voltage of -15 kV and the gas velocity of 0.062–0.124 m/s. For continuous tests of the WESP for 6 h in the laboratory with wall-cleaning water, only a slight decrease of less than 2% in the collection efficiency for SiO_2 particles ($40 \leqslant d_p \leqslant 8100$ nm) was found because the scrubbing water could clean collection and discharge electrodes effectively to maintain a high collection efficiency. High particle collection efficiency was also found in the long-term field tests, in which the collection efficiencies of the WESP for SiO_2 particles with $40 \leqslant d_p \leqslant 8100$ nm could be maintained to be greater than the total collection efficiencies of the WESP were found to maintain greater than 98.9% and 97.3% for continuous operation for 35 and 22 day at fab A and fab B, respectively.

An empirical equation was derived to predict the particle collection efficiency of the WESP when the gas velocity is lower than or equal to 0.5 m/s. The comparison of predicted particle collection efficiencies by the present model with the present and previous experimental data showed good agreement with a deviation of <3% and <6%, respectively. It is expected that the empirical equation can facilitate the design and scale-up of the WESP for mitigate the emission of nanoparticles and fine particles efficiently.

Acknowledgements

The financial support of Green Energy and Environment Research Laboratories in the Industrial Technology Research Institute is gratefully acknowledged.

References

[1] S. Nakao, T. Suzuki, T. Sugawara, T. Tsuru, S. Kimura, Preparation of microporous membranes by TEOS/O_3 CVD in the opposing reactants geometry, Micropor. Mesopor. Mater. 37 (2000) 145–152.
[2] Y. Kajikawa, T. Tsuchiya, S. Nado, H. Komiyama, Incubation time during the CVD of Si onto SiO_2 from silane, Chem. Vapor Depos. 10 (2004) 128–133.
[3] S.J. Khatib, S.T. Oyama, K.R. Souza, F.B. Noronha, Review of silica membranes for hydrogen separation prepared by chemical vapor deposition, in: S.T. Oyama, S.M. Stagg-Williams (Eds.), Inorganic Polymeric and Composite Membranes: Structure-Function and other Correlations, Elsevier, Amsterdam, 2011, pp. 25–60. Chapter 2.
[4] S.J. Yu, S.N. Li, S.Y. Yan, J.N. Hsu, T.M. Chen, Current technical development of domestic local scrubber, Chem. Technol. 65 (2008) 70–77.
[5] S.J. Yu, T.M. Chen, C.H. Leu, S.Y. Yan, Operation evaluation and practice analysis of environmental protection equipments for high-tech and green energy industries, J. CIE Assoc. 84 (2011) 88–98.
[6] C.J. Tsai, C.C. Miao, H.C. Lu, White smoke emission from a semiconductor manufacturing plant, Environ. Int. 23 (1997) 489–496 (in Chinese).
[7] C.A. Pope III, R.T. Burnett, G.D. Thurston, M.J. Thun, E.E. Calle, D. Krewski, J.J. Godleski, Cardiovascular mortality and long-term exposure to particulate air pollution: epidemiological evidence of general pathophysiological pathways of disease, Circulation 109 (2004) 71–77.
[8] S.B. Lovern, J.R. Strickler, R. Klaper, Behavioral and physiological changes in Daphnia magna when exposed to nanoparticle suspensions (titanium dioxide, nano-C_{60}, and $C_{60}H_xC_{70}H_x$), Environ. Sci. Technol. 41 (2007) 4465–4470.
[9] G. Oberdörster, A. Elder, A. Rinderknecht, Nanoparticles and the brain: cause for concern?, J Nanosci. Nanotechnol. 9 (2009) 4996–5007.
[10] I. Brüske, R. Hampel, M.M. Socher, R. Rückerl, A. Schneider, J. Heinrich, G. Oberdörster, H.E. Wichmann, A. Peters, Impact of ambient air pollution on the differential white blood cell count in patients with chronic pulmonary disease, Inhal. Toxicol. 22 (2010) 245–252.
[11] S.H. Huang, C.C. Chen, Loading characteristics of a miniature wire-pate electrostatic precipitator, Aerosol Sci. Technol. 37 (2003) 109–121.
[12] S. Tekasakul, M. Tantichaowanan, Y. Otani, P. Kuruhongsa, P. Tekasakul, Removal of soot particles in rubber smoking chamber by electrostatic precipitator to improve rubber sheet color, Aerosol Air Qual. Res. 6 (2006) 1–14.
[13] G.Y. Lin, C.J. Tsai, S.C. Chen, T.M. Chen, S.N. Li, An efficient single-stage wet electrostatic precipitator for fine and nanosized particle control, Aerosol Sci. Technol. 44 (2010) 38–45.
[14] P.V. Bush, Study of rapping reentrainment emissions from a pilot-scale electrostatic precipitator, Environ. Sci. Technol. 18 (1984) 699–708.
[15] T. Yamamoto, M. Mieno, K. Shibata, Studies of rapping reentrainment from electrostatic precipitators, in: Proc. 7th International Conference on Electrostatic Precipitation, 1998, pp. 163–170.
[16] T. Ferge, J. Ferge, R. Zimmermann, Particle collection efficiency and particle re-entrainment of an electrostatic precipitator in a sewage sludge incineration plant, Environ. Sci. Technol. 38 (2004) 1545–1553.
[17] C.L. Chang, H. Bai, An experimental study on the performance of a single discharge wire-plate electrostatic precipitator with back corona, J. Aerosol Sci. 30 (1999) 325–340.
[18] C. Ruttanachot, Y. Tirawanichakul, P. Tekasakul, Application of electrostatic precipitator in collection of smoke aerosol particles from wood combustion, Aerosol Air Qual. Res. 11 (2011) 90–98.

[19] K.H. Yoo, J.S. Lee, M.D. Oh, Charging and collection of submicron particles in two-stage parallel-plate electrostatic precipitators, Aerosol Sci. Technol. 27 (1999) 308–323.
[20] S.H. Huang, C.C. Chen, Ultrafine aerosol penetration through electrostatic precipitators, Environ. Sci. Technol. 36 (2002) 4625–4632.
[21] G.Y. Lin, T.M. Chen, C.J. Tsai, A modified Deutsch–Anderson equation for predicting the nanoparticle collection efficiency of electrostatic precipitators, Aerosol Air Qual. Res. 12 (2012) 697–706.
[22] Y. Zhuang, Y. Kim, T. Lee, P. Biswas, Experimental and theoretical studies of ultra-fine particle behavior in electrostatic precipitators, J. Electrostat. 48 (2000) 245–260.
[23] P. Kulkarni, N. Namiki, Y. Otani, P. Biswas, Charging of particles in unipolar coronas irradiated by in-situ soft X-rays: enhancement of capture efficiency of ultrafine particles, J. Aerosol Sci. 33 (2002) 1279–1296.
[24] G.Y. Lin, C.J. Tsai, Numerical modelling of nanoparticle collection efficiency of single-stage wire-in-plate electrostatic precipitators, Aerosol Sci. Technol. 44 (2010) 1122–1130.
[25] J. Agarwal, G. Sem, Continuous-flow, single-particle-counting condensation nucleus counter, J. Aerosol Sci. 11 (1980) 343–357.
[26] C.J. Tsai, C.H. Huang, C.H. Lin, Y.M. Wang, S.N. Li, Z.X. Wu, F.C. Wang, An efficient venture scrubber system to remove submicron particles in exhaust gas, J. Air Waste Manage. Assoc. 55 (2005) 319–325.
[27] C.H. Huang, C.J. Tsai, Y.M. Wang, Control efficiency of submicron particles by an efficient venture scrubber system, J. Environ. Eng. 133 (2007) 454–461.
[28] L. Yang, J. Bao, J. Yan, J. Liu, S. Song, F. Fan, Removal of fine particles in wet flue gas desulfurization system by heterogeneous condensation, Chem. Eng. J. 156 (2010) 25–32.
[29] F.J. Gutiérrez Ortiz, B. Navarrete, L. Cañadas, Dimensional analysis for assessing the performance of electrostatic precipitators, Fuel Process. Technol. 91 (2010) 1783–1793.
[30] S. Matts, P.O. Öhnfeldt, Efficient gas cleaning with SF electrostatic precipitator, Fläkt 1 (1964) 93–110.
[31] P.A. Lawless, Particle charging bounds, symmetry relations, and an analytic charging rate model for the continuum regime, J. Aerosol Sci. 27 (1996) 191–215.
[32] P. Saiyasitpanich, T.C. Keener, S.J. Khang, M. Lu, Removal of diesel particulate matter (DPM) in a tubular wet electrostatic precipitator, J. Electrostat. 65 (2007) 618–624.
[33] W.C. Hinds, Aerosol Technology, John Wiley & Sons, New York, 1999. pp. 323–330.
[34] C. Riehle, F. Löffier, Electrical similarity concerning particle transport in electrostatic precipitators, J. Electrostat. 29 (1992) 147–165.
[35] J. Richards, Control of Particulate Matter Emissions, APTI course 413, third ed., vol. 5, EPA, Washington, DC, 2000, pp. 5-20–5-24.